

Clinical Study

Assessing Response to Radiation Therapy Treatment of Bone Metastases: Short-Term Followup of Radiation Therapy Treatment of Bone Metastases with Diffusion-Weighted Magnetic Resonance Imaging

Salvatore Cappabianca,¹ Raffaella Capasso,¹ Fabrizio Urraro,¹ Andrea Izzo,¹ Antonio Raucci,¹ Rossella Di Franco,² and Antonio Rotondo¹

¹ Department of Internal Clinical and Experimental Medicine, Second University of Naples, Piazza Miraglia 4, 80100 Naples, Italy

² Assisential Department of Radiology, Radiotherapy and Nuclear Medicine, Second University of Naples, Piazza Miraglia 4, 80100 Naples, Italy

Correspondence should be addressed to Raffaella Capasso; dott.ssacapasso@gmail.com

Received 17 October 2013; Revised 8 January 2014; Accepted 17 February 2014; Published 26 March 2014

Academic Editor: Samer Ezziddin

Copyright © 2014 Salvatore Cappabianca et al. This is an open access article distributed under the Creative Commons Attribution License, which permits unrestricted use, distribution, and reproduction in any medium, provided the original work is properly cited.

This study examined the usefulness of diffusion-weighted (DW) Magnetic Resonance Imaging (MRI) in monitoring bone metastases response to radiation therapy in 15 oligometastatic patients. For each metastasis, both mean apparent diffusion coefficient (ADC) changes and high *b*-value DW metastasis/muscle signal intensity ratio (SIR) variations were evaluated at 30 ± 5 days and 60 ± 7 days after the end of treatment. On baseline DW-MRI, all bone metastases were hyperintense and had signal intensities higher than normal bone marrow on calculated ADC maps. At follow-up evaluations, 4 patterns of response were identified: (I) decreased high *b*-value DW SIR associated with increased mean ADC (83.3% of cases); (II) increased mean ADC with no change of high *b*-value DW SIR (10% of cases); (III) decreased both high *b*-value DW SIR and mean ADC (3.3% of cases); (IV) a reduction in mean ADC associated with an increase in high *b*-value DW SIR compared to pretreatment values (3.3% of cases). Patterns (I) and (II) suggested a good response to therapy; pattern (III) was classified as indeterminate, while pattern (IV) was suggestive of disease progression. This pattern approach may represent a useful tool in the differentiation between treatment-induced necrosis and highly cellular residual tumor.

1. Introduction

Bone metastases occur from 30% to 70% of all patients suffering from cancer and commonly involve the axial skeleton [1, 2]. Breast, prostate, and lung cancers represent the main sources of bone metastases, with prostate and lung cancers being most common in males and breast cancer being most common in females [2]. Once bony metastases occur, cancer cure becomes impossible and in these cases radiation therapy, associated or not with systemic chemotherapy, may be performed for palliative intent [1, 3]. Therapy goals are to delay progression, palliate symptoms, improve quality of

life, and achieve any possible survival benefit [3]. Currently, there are no universally accepted methods for evaluating the response to treatment, making it difficult to give patient the optimal management to minimize radiation dose and prevent recurrences [1, 3]. Bone scintigraphy (^{99m}Tc -methylene diphosphonate-MDP-bone scans) with plain radiographs or cross-sectional imaging, such as Computed Tomography (CT) or Magnetic Resonance Imaging (MRI), and sometimes ^{18}F -fluoride Positron Emission Tomography (PET)/CT remain the commonest imaging methods, complementing one another in order to characterize and follow up bone marrow metastases [1, 3, 4]. Although conventionally used, none

of these imaging modalities combines satisfactory quantitative assessment of treatment response with good anatomical resolution. Some further limitations are represented by the flare phenomenon of radionuclide bone scanning and by the low specificity of conventional spin-echo MRI sequences [1, 3, 4]. In the context of bone marrow assessment of metastatic disease, diffusion-weighted (DW) MRI is increasingly being used because DW signal is sensitive to bone marrow cell density, water content, and bone marrow perfusion [5]. DW-MRI has the potential to provide new and previously unobtainable quantitative measures of metastatic lesions response, without use of extrinsic contrast agents or exposure to ionizing radiation [3]. Then, DW-MRI is being applied for monitoring response to radiation therapy and appears to be able to predict treatment response [2, 6]. In our study, we examined the usefulness of DW-MRI for monitoring the early response to radiation therapy of metastatic disease through the evaluation of response patterns based on both apparent diffusion coefficient (ADC) changes and, respectively, high *b*-value DW signal variations about 30 and 60 days after the end of treatment.

2. Material and Methods

2.1. Patients. Between June 2011 and December 2012, we prospectively examined 18 (7 females, 11 males) oligometastatic (with 1 bone metastasis) patients who underwent external beam radiotherapy with a conventional scheme of 30 Gray (Gy) delivered in ten 3 Gy fractions at our institution [7]. These 18 patients were selected among all (47) metastatic patients in the care of our institution, excluding the ones (12) who took bisphosphonates or hydroxyapatite derivatives in order to avoid misinterpretations of MRI findings due to medical therapy effects [8]. All selected patients had both documented metastases to other organs and metastases to the axial skeleton documented by radionuclide bone scanning; so, the bony lesions with typical MRI findings were assumed to represent metastases in all patients. Only patients who performed MRI evaluations at correct timing and with suitable signal-to-noise ratio were included in the study. Then, 15 patients (3 females and 12 males) spinal or pelvic bone metastases affected (13 and 2 cases, resp.) were finally included in this study. Patient age ranged from 30 to 81 years, with an average age of 51.7 years. Primary neoplasms were as follows: invasive ductal carcinoma of the breast ($n = 1$), adenocarcinoma of the prostate ($n = 8$), renal cell carcinoma ($n = 1$), adenocarcinoma of the colon ($n = 1$), lung cancer ($n = 3$), and hepatocellular carcinoma ($n = 1$).

2.2. Imaging. Patients were imaged at baseline (within 7 days before the beginning of radiotherapy), 30 ± 5 days, and 60 ± 7 days after the end of the therapy including standard anatomic and diffusion-weighted sequences. MRI was performed at 1.5 Tesla (T) superconductive scanner (Symphony, Siemens, Erlangen, Germany) using an external coil array with subjects positioned supine. T1- and T2-weighted (w) sequences were acquired in sagittal or axial plane. DW images were acquired using the following parameters: repetition time (TR) =

5400 ms, echo time (TE) = 79 ms, *b*-value: 0, 50 s/mm² (low), 250 s/mm² (medium), and 750 s/mm² (high). ADC maps were calculated based on images without diffusion gradient (*b* = 0; T2) and low, medium, and high *b*-values DW images, thanks to the Siemens imaging unit software by using a monoexponential fit of all *b*-factor images at each measurement time point. For each metastasis was categorized the signal intensity on T1- and T2-w images as hypo-, iso-, or hyperintense relative to the areas of presumed normal marrow. To calculate the mean ADC for each lesion, a single circular region of interest (ROI) was drawn over each tumor-bearing section on the ADC map image where the metastasis seemed to have the major extent, using T1-w MR sequences to aid placement, covering to the utmost the lesion and avoiding artefacts. ROIs were then copied onto DW images for all *b*-values. For each lesion, another ROI of equal size was also positioned on muscular tissue (paravertebral or gluteal according to the site of the metastases) considered as reference tissue in order to calculate the mean metastasis/muscle signal intensity ratio (SIR). Maintaining the same positions and sizes of ROIs on follow-up MR studies, the findings obtained 30 ± 5 days and 60 ± 7 days after therapy were compared with those registered before radiotherapy.

3. Results

All bone metastases before therapy were hypointense to normal bone marrow on T1-weighted spin-echo images and hyperintense (9 cases) or hypointense (6 cases) on T2-weighted spin-echo images. Follow-up T1- and T2-w MRI findings revealed no interval change of signal intensities (Table 1). On baseline DW-MRI, all bone metastases were hyperintense (the lower the *b*-value the higher the signal intensity) (Figure 1) and had signal intensities higher than normal bone marrow on calculated ADC maps. Table 2 shows metastasis/muscle SIR and mean ADC variations during follow-up examinations. At first follow-up, considering both lesion-by-lesion high *b*-value DW SIR and mean ADC changes, three response patterns were identified: (I) decreased high *b*-value DW SIR associated with increased mean ADC (13 cases); (II) increased mean ADC with no change of high *b*-value DW SIR (1 case: patient number 1 on Table 2); (III) decreased both high *b*-value DW SIR and mean ADC (1 case: patient number 9 on Table 2) [3]. At second follow-up, in addition to the first pattern (12 cases) and the second one (2 cases: patients number 6 and number 7 on Table 2), the following was also observed: (IV) a reduction of mean ADC associated with an increase in high *b*-value DW SIR compared to pretreatment values (1 case: patient number 9 on Table 2).

4. Discussion

Bone expansive processes were known since the dawn of time and skeletal metastases are the most common malignancies among all bone tumors [2, 9]. Detection of bone metastases is essential for accurate staging and optimal treatment of

TABLE 1: The table shows the appearance of metastases on T1- and T2-weighted spin-echo images before therapy and at follow-up MRI evaluations. No changes were noticed.

Before therapy		Signal intensities			
T1-w	T2-w	T1-w	30 ± 5 days	T1-w	60 ± 7 days
Hypo	Hyper	Hypo	Hyper	Hypo	Hyper
Hypo	Hyper	Hypo	Hyper	Hypo	Hyper
Hypo	Hyper	Hypo	Hyper	Hypo	Hyper
Hypo	Hyper	Hypo	Hyper	Hypo	Hyper
Hypo	Hyper	Hypo	Hyper	Hypo	Hyper
Hypo	Hyper	Hypo	Hyper	Hypo	Hyper
Hypo	Hypo	Hypo	Hypo	Hypo	Hypo
Hypo	Hyper	Hypo	Hyper	Hypo	Hyper
Hypo	Hyper	Hypo	Hyper	Hypo	Hyper
Hypo	Hyper	Hypo	Hyper	Hypo	Hyper
Hypo	Hypo	Hypo	Hypo	Hypo	Hypo
Hypo	Hypo	Hypo	Hypo	Hypo	Hypo
Hypo	Hypo	Hypo	Hypo	Hypo	Hypo
Hypo	Hypo	Hypo	Hypo	Hypo	Hypo

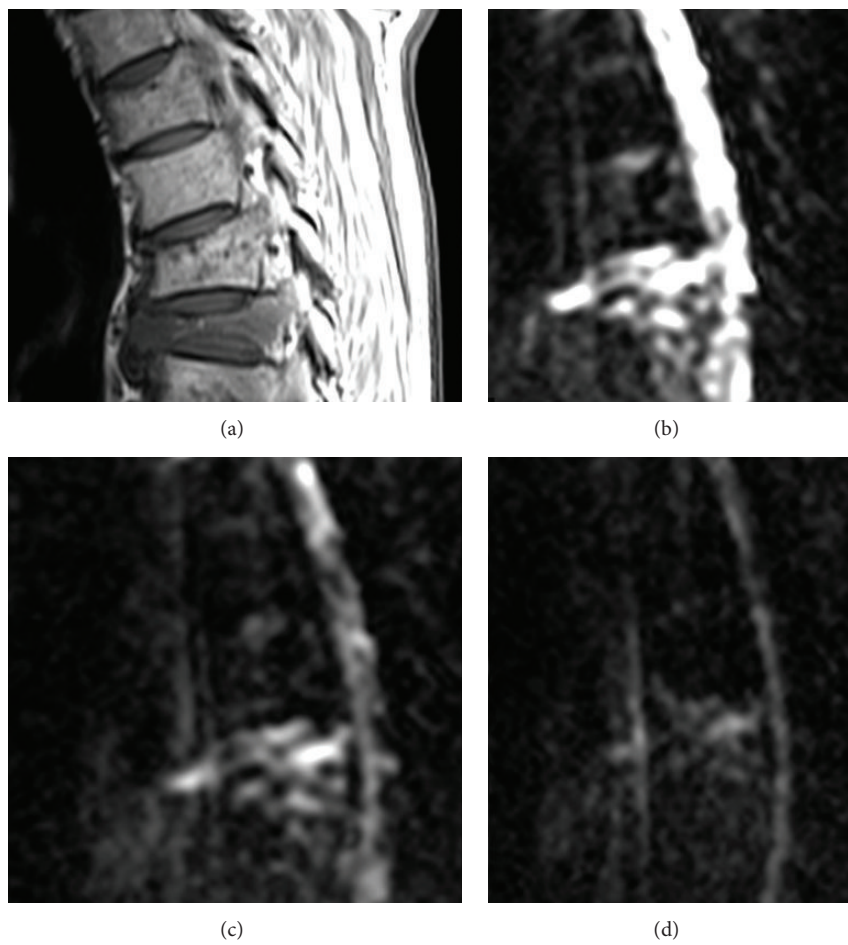


FIGURE 1: MRI: the bone metastases hypointense on T1-weighted sagittal MR images show a progressive reduction of signal intensity on DW images obtained using low (b), medium (c), and high (d) b -value.

TABLE 2: The table shows for each metastasis the mean ADC and metastasis/muscle SIRs of DW-MRI examinations performed before and after therapy. ADC mean values reached after therapy are also presented as percent variations from corresponding ADC value registered before therapy. Response patterns are discussed in the text.

Patient	DW metasis/muscle SIR variations and mean ADC changes										% ADC increase			
	Before therapy				30 ± 5 days				60 ± 7 days				(× 10 ⁻⁵ mm ² /s ± SD)	
	b-value	b-value	(× 10 ⁻⁵ mm ² /s ± SD)	ADC	b-value	b-value	(× 10 ⁻⁵ mm ² /s ± SD)	ADC	b-value	b-value	(× 10 ⁻⁵ mm ² /s ± SD)	ADC	30 ± 5 days	60 ± 7 days
1	2.29	1.5	0.89	113.56 ± 16.75	3.5	1.65	0.9	131.71 ± 9.27	2.55	1.08	0.46	195.56 ± 10.20	15.9	72.2
2	1.89	1.52	1.08	72.44 ± 12.58	3.44	1.69	0.96	130.08 ± 6.88	3.51	1.45	0.57	172.52 ± 17.24	81	140
3	1.64	1.41	0.91	86.87 ± 16.16	3.24	1.37	0.84	101.51 ± 8.93	2.27	0.94	0.5	165.04 ± 14.30	17.3	90.2
4	5.98	3.35	2.71	115.08 ± 4.10	9.4	3.39	2.15	191.92 ± 10.37	9.66	3.01	2.05	211.00 ± 6.73	66.7	83.3
5	4.08	1.74	1.47	184.00 ± 29.27	3.61	1.65	1.28	201.23 ± 23.45	3.95	1.82	1.04	247.18 ± 19.55	9.3	34.3
6	2.73	1.73	1.22	145.62 ± 13.75	5.17	1.91	0.78	171.47 ± 10.04	4.56	3.3	0.8	184.65 ± 73.34	17.7	26.8
7	2.11	0.37	0.26	104.44 ± 31.15	2.21	0.55	0.22	128.29 ± 17.95	2.2	0.49	0.22	160.19 ± 11.62	22.8	53.4
8	2.02	1.5	0.95	76.54 ± 2.69	1.94	1.12	0.78	130.08 ± 4.44	1.63	1.34	0.97	156.92 ± 3.57	70.5	104.5
9	1.87	0.92	0.45	146.38 ± 7.61	1.17	0.6	0.32	128.46 ± 2.54	1.15	0.56	0.49	89.00 ± 12.59	-12.2	-39.2
10	1.59	0.77	0.38	95.46 ± 11.10	0.8	0.44	0.36	123.50 ± 17.19	0.75	0.41	0.32	196.71 ± 10.60	29.4	106.0
11	1.47	0.77	0.75	112.69 ± 17.21	0.97	0.81	0.51	123.62 ± 11.49	1.81	0.88	0.48	153.34 ± 19.09	9.7	36.1
12	3.09	1.62	1.22	143.38 ± 18.89	2.16	0.88	0.7	176.62 ± 4.27	2.11	0.95	0.51	181.50 ± 11.03	23.2	26.6
13	2.00	1.17	0.87	106.92 ± 15.46	1.53	0.87	0.59	141.00 ± 18.59	1.37	0.9	0.37	150.31 ± 7.98	31.9	40.6
14	1.54	1.29	1.05	122.15 ± 8.42	1.51	1.28	0.62	137.00 ± 9.36	1.07	0.86	0.48	150.37 ± 8.02	12.2	23.1
15	2.64	2.4	1.4	106.89 ± 12.25	1.6	0.88	0.4	165.70 ± 19.16	1.32	0.75	0.23	183.57 ± 14.32	55.0	71.7
Mean	2.46	1.47	1.04	115.49 ± 14.49	2.81	1.27	0.68	145.43 ± 11.59	2.66	1.25	0.53	173.19 ± 11.61	30.0	57.9

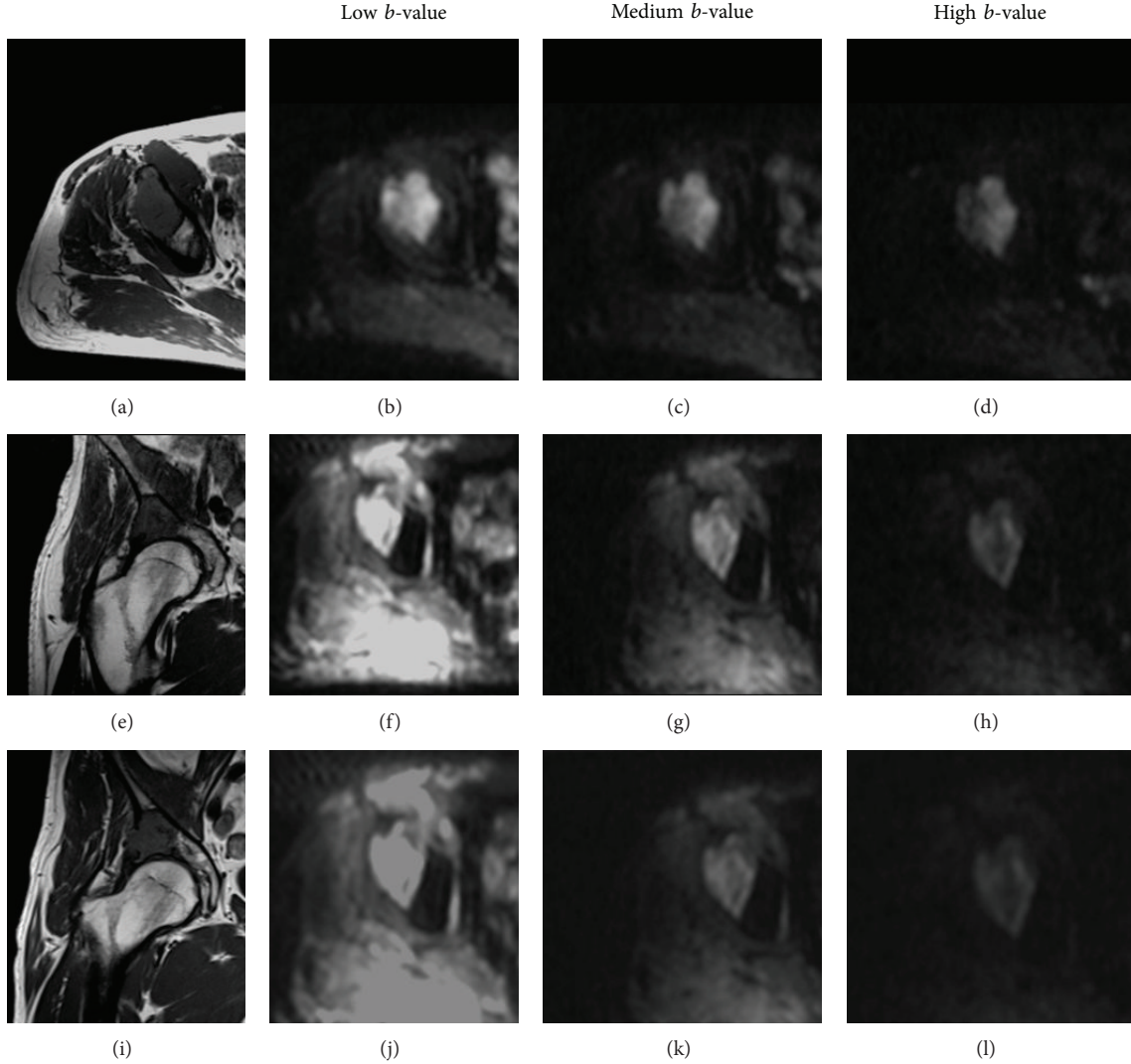


FIGURE 2: MRI: before therapy ((a), (b), (c), (d)), 33 days after therapy ((e), (f), (g), (h)), and 64 days after therapy ((i), (j), (k), (l)). The bone metastases hypointense on T1-weighted images ((a), (e), (i)) appear similarly hyperintense on DW images obtained using low b -value ((b), (f), (l)), whilst the inner signal intensity variation after treatment is better highlighted comparing with images obtained using high b -value ((d), (h), (l)).

neoplastic patients, and it is out of question that MRI is an excellent method for assessing the bone marrow [2, 10].

4.1. T1- and T2-Weighted Images. Thanks to the natural contrast created by the relatively high signal intensity of normal adult fatty bone marrow, metastases result hypointense on noncontrast T1-w images reflecting replacement of fatty bone marrow, increased water content, and hypercellularity. However, a hypointensity on T1-w images is not specific to bone metastases because any replacement of the bone marrow appears hypointense in comparison to normal marrow [10, 11]; then, T1-w images alone are not able to discriminate between metastatic lesion and benign vertebral fracture [12]. In our study, symptomatic bone marrow lesions, hypointense in T1-w images and related to radionuclide increased uptake

at bone scan, were diagnosed as metastases. T2-w images do not add further information in differential diagnosis between metastases and other bone marrow focal lesions, because of wide variability of bone marrow metastases signal [10, 13]. Byun et al. reported that follow-up MR images obtained at least 1 month after therapy showed persistent abnormal hypointensity on T1-w MR images and variable signal intensities on T2-w MRI [13]. These data are in agreement with our results and support the observation that conventional spin-echo T1- or T2-w MRI may not be conclusive for monitoring the therapy response (Figures 2(a), 2(e), 2(i), 3(g), 3(h), and 3(i)) [13].

4.2. DWI. Whole-body DW imaging (WB-DWI) is emerging as an accurate bone marrow assessment tool for detection and

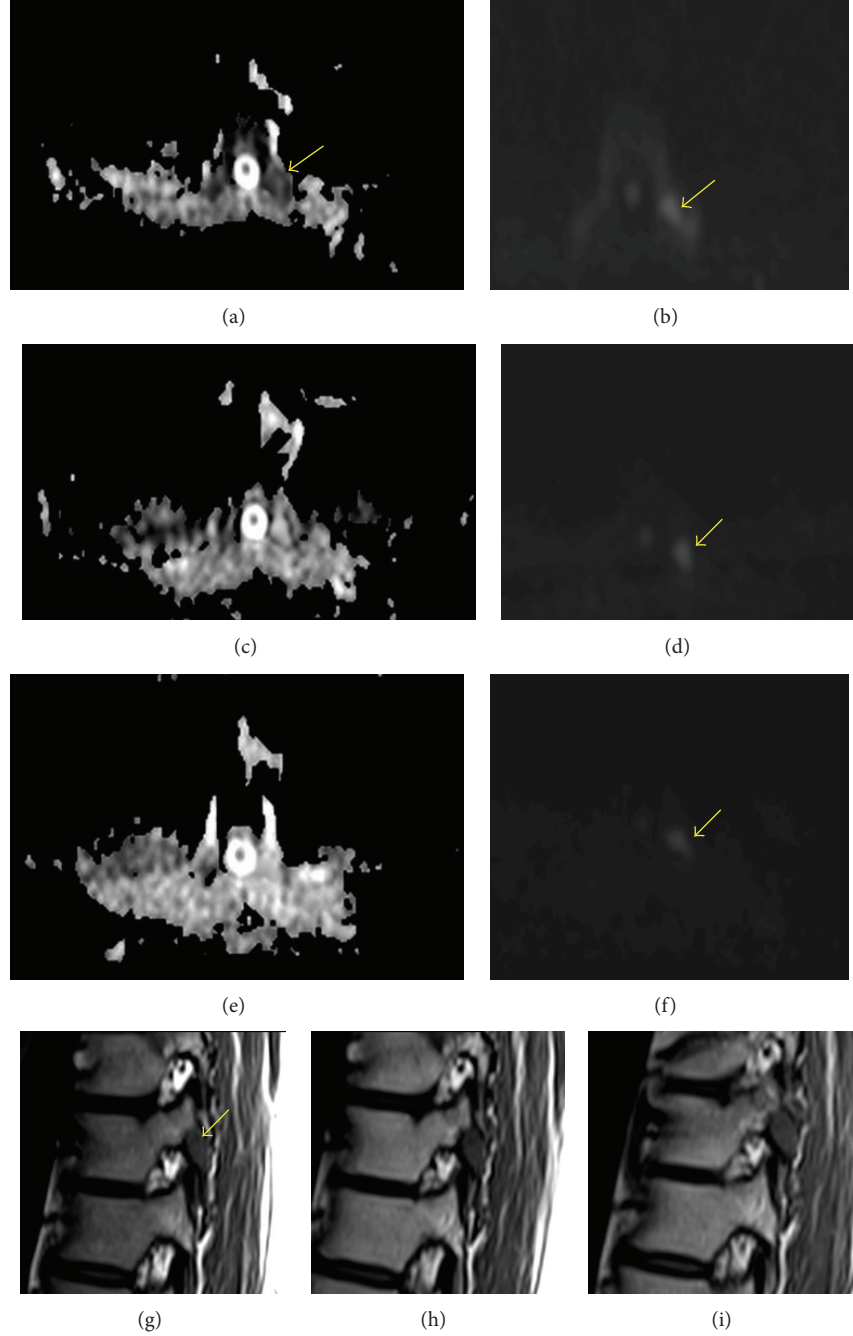


FIGURE 3: MRI: before therapy ((a), (b), (g)), 29 days after therapy ((c), (d), (h)), and 58 days after therapy ((e), (f), (i)). Pattern of good response to radiation therapy: tumor necrosis determines increased water diffusivity manifested as higher ADC SIR ((a): 1.11; (c): 2.01; (e): 2.64) and decreased hyperintensity on high b -value images (SIR (b): 1.08; (d): 0.96; (f): 0.57). Lesion remains hypointense on T1-weighted MRI ((g), (h), (i)).

therapy monitoring of bone metastases [3, 7, 14, 15]. Indeed, cellularity of bone marrow correlates with DWI signal intensity of the bone [3]. Generally, lytic bony metastases are better seen than sclerotic ones, because for the latter, despite the increased hypercellularity, the extracellular space likely remains normal (or near normal), and the water it contains is relatively free to have Brownian (random) motion, leading to spin dephasing and loss of signal on DWI [6, 10, 12, 16, 17]. As a result, purely sclerotic bone metastases that are not

visible on DWI are not assessable for response [3, 6]. One patient with prostate metastases was not included in our study because the vertebral lesion was difficult to identify on DWI due to its very low signal and the resulting insufficient signal-to-noise ratio on increased b -value DWI. The signal attenuation due to diffusion plays only a minor role in the case of a smaller b -value [12]. Moreover, Castillo et al. reported that T2-shine through effects can be removed by increasing the strength of b -value gradients, also reducing the signal to

noise ratio (Figure 2) [3, 10, 12]. Therefore, for our patients, DWI was also obtained with high *b*-value striking out false-positive focal increases in signal intensity on DWI for T2-w hyperintense metastases. In this study, metastases appeared hyperintense compared with normal bone marrow on high *b*-value DWI and ADC maps obtained before therapy. This aspect is in agreement with previous reports, which described a minimal diffusion and low ADC value of normal bone marrow [13, 18].

4.3. Assessment of Response to Treatment. Quantification of the amount of increased ADC values in tumor regions experiencing a loss of cellular density can be used to assess the treatment effects. Water mobility within a tumor will increase over time following effective treatment, as represented by an increase in MRI-quantified ADC values, with the magnitude of the change related to the effectiveness of the therapy [19, 20]. Messiou et al. reported that mean ADC alone is not an appropriate measure of response in bone metastases because of the heterogeneity of changes in ADC [4]. Messiou et al. noted that rising ADC in bone metastases is common in both responding and progressing patients while a fall in ADC can be encountered because of returning marrow fat in responders and the tumor repopulation of lytic lesions in progressors [4]. On the other hand, Byun et al. concluded that DW-MRI shows that, with successful therapy, there is decreased signal intensity of metastatic disease of the vertebral bone marrow [13]. Thus, we considered both lesion-by-lesion DW signal intensity and mean ADC value changes identifying different response patterns.

4.4. Response Patterns

4.4.1. Pattern I (83.3% of Cases). The decrease of high *b*-value DW SIR associated with an increased mean ADC suggests a good response to therapy because when bone marrow disease is treated successfully, then tumor necrosis determines increased membrane permeability and breakdown of the cell membrane and the intracellular structure resulting in increased water diffusivity manifested as higher ADC values and decreased intensity on high *b*-value images (Figure 3) [3, 21].

4.4.2. Pattern II (10% of Cases). A successful response to therapy may be supposed even when the rise in ADC values is associated with no high *b*-value DW SIR changes. This pattern has been noted occasionally in solid metastatic neoplasms [6]. However, because ADC value alone does not ensure a correct ruling, serial follow-up studies are needed to reveal the true nature of response then observing the time course of changes [3, 4, 6]. In our study, the case observed 32 days after therapy (patient number 1), at successive evaluation, showed the pattern of good response: further increase of mean ADC and reduction of high *b*-value DW SIR that became lower than pretreatment one. The other two cases (patients number 6 and number 7) showing this response pattern—no further decrease of high *b*-value DW SIR together with an additional ADC rise compared

to previous evaluation—were observed at second follow-up evaluation 60 ± 7 days after therapy. Although ADC value can increase even if bone metastases do not respond to therapy, in our cases mean ADC rises were progressive and considerable, being the growth of almost a quarter (26.8%) and of about a half (53.4%) of initial values, respectively; thereof, we could lean towards a good response to therapy [3].

4.4.3. Pattern III (3.3% of Cases). The decrease of both high *b*-value DW SIR and mean ADC observed in 1 case 31 days after therapy (patient number 9) represents a rare pattern [6]. A reduction of high *b*-value DW signal may be caused by bone sclerosis within initially lytic disease, fibrotic reaction, or tumor necrosis, whilst a fall in ADC value may be due to not only returning marrow fat in responders but also due to tumor repopulation in progressors [3, 4]. Since this pattern can be seen in responders and nonresponders, these appearances should be considered as indeterminate [3].

4.4.4. Pattern IV (3.3% of Cases). On successive control evaluation, the indeterminate lesion (patient number 9) showed a reduction of mean ADC with an increase of high *b*-value DW SIR. This pattern is suggestive of disease progression. Tumor growth causes an increase of bone marrow cellularity, which displaces fat cells and enlarges the vascularity of the bone marrow leading to an increase of SIR on high *b*-value images. This increase of high *b*-value signal intensity rules out the presence of blastic cells tissue within lytic metastasis because it determines a loss in signal intensity as observed during many systemic treatments for osteolytic disease working by inhibiting osteoclastic action (bisphosphonates or hydroxyapatite derivatives), thus converting osteolytic lesions to sclerotic ones [6]. In addition, once all bone marrow fat cells are displaced, the compact accumulation of neoplastic cells confined in a fixed marrow space causes ADC reductions [3, 13].

5. Conclusions

This study has several limits, first of all the low number of patients. Moreover, the identified patterns are only suggestive of the type of the response to therapy but are not able to replace the biopsy. Despite these limitations, our investigation revealed that the matched evaluation of both high *b*-value DW signal intensity and mean ADC value changes may be a useful tool to explore underlying biophysical properties of skeletal metastases and early therapy-induced effects. The identification of the pattern of response to therapy could play a key role in the therapy assessments of patients with metastatic disease allowing differentiation between areas of treatment-induced necrosis and highly cellular residual tumor.

Abbreviations

ADC: Apparent diffusion coefficient

MR: Magnetic Resonance

MRI: Magnetic Resonance Imaging

- DW: Diffusion weighted
 DW-MRI: Diffusion-weighted Magnetic Resonance Imaging
 SIR: Signal intensity ratio.

Conflict of Interests

The authors declare that there is no conflict of interests regarding the publication of this paper.

References

- [1] W. M. Byun, S. O. Shin, Y. Chang, S. J. Lee, J. Finsterbusch, and J. Frahm, "Diffusion-weighted MR imaging of metastatic disease of the spine: assessment of response to therapy," *American Journal of Neuroradiology*, vol. 23, no. 6, pp. 906–912, 2002.
- [2] J. Choi and M. Raghavan, "Diagnostic imaging and image-guided therapy of skeletal metastases," *Cancer Control*, vol. 19, no. 2, pp. 102–112, 2012.
- [3] A. R. Padhani and A. Gogbachian, "Bony metastases: assessing response to therapy with whole-body diffusion MRI," *Cancer Imaging*, vol. 11, pp. S129–S145, 2011.
- [4] C. Messiou, D. J. Collins, S. Giles, J. S. de Bono, D. Bianchini, and N. M. de Souza, "Assessing response in bone metastases in prostate cancer with diffusion weighted MRI," *European Radiology*, vol. 21, no. 10, pp. 2169–2177, 2011.
- [5] A. Biffar, O. Dietrich, S. Sourbron, H.-R. Duerr, M. F. Reiser, and A. Baur-Melnyk, "Diffusion and perfusion imaging of bone marrow," *European Journal of Radiology*, vol. 76, no. 3, pp. 323–328, 2010.
- [6] A. R. Padhani, D.-M. Koh, and D. J. Collins, "Whole-body diffusion-weighted MR imaging in cancer: current status and research directions," *Radiology*, vol. 261, no. 3, pp. 700–718, 2011.
- [7] N. Nakamura, N. Shikama, H. Wada et al., "Patterns of practice in palliative radiotherapy for painful bone metastases: a survey in Japan," *International Journal of Radiation Oncology Biology Physics*, vol. 83, no. 1, pp. e117–e120, 2012.
- [8] L. S. Loftus, S. Edwards-Bennett, and G. H. Sokol, "Systemic therapy for bone metastases," *Cancer Control*, vol. 19, no. 2, pp. 145–153, 2012.
- [9] G. Colella, S. Cappabianca, G. Gerardi, and F. Mallegni, "Homo neanderthalensis; first documented benign intraosseous tumor in maxillofacial skeleton," *Journal of Oral and Maxillofacial Surgery*, vol. 70, no. 2, pp. 373–375, 2012.
- [10] M. Castillo, A. Arbelaez, J. K. Smith, and L. L. Fisher, "Diffusion-weighted MR imaging offers no advantage over routine non-contrast MR imaging in the detection of vertebral metastases," *American Journal of Neuroradiology*, vol. 21, no. 5, pp. 948–953, 2000.
- [11] C. Ricci, M. Cova, Y. S. Kang et al., "Normal age-related patterns of cellular and fatty bone marrow distribution in the axial skeleton: MR imaging study," *Radiology*, vol. 177, no. 1, pp. 83–88, 1990.
- [12] O. Oztekin, E. Ozan, Z. H. Adibelli, G. Unal, and Y. Abali, "SSH-EPI diffusion-weighted MR imaging of the spine with low b values: is it useful in differentiating malignant metastatic tumor infiltration from benign fracture edema?" *Skeletal Radiology*, vol. 38, no. 7, pp. 651–658, 2009.
- [13] W. M. Byun, S. O. Shin, Y. Chang, S. J. Lee, J. Finsterbusch, and J. Frahm, "Diffusion-weighted MR imaging of metastatic disease of the spine: assessment of response to therapy," *American Journal of Neuroradiology*, vol. 23, no. 6, pp. 906–912, 2002.
- [14] K. Nakanishi, M. Kobayashi, K. Nakaguchi et al., "Whole-body MRI for detecting metastatic bone tumor: diagnostic value of diffusion-weighted images," *Magnetic Resonance in Medical Sciences*, vol. 6, no. 3, pp. 147–155, 2007.
- [15] L.-M. Wu, H.-Y. Gu, J. Zheng et al., "Diagnostic value of whole-body magnetic resonance imaging for bone metastases: a systematic review and meta-analysis," *Journal of Magnetic Resonance Imaging*, vol. 34, no. 1, pp. 128–135, 2011.
- [16] A. Baur, A. Huber, B. Ertl-Wagner et al., "Diagnostic value of increased diffusion weighting of a steady-state free precession sequence for differentiating acute benign osteoporotic fractures from pathologic vertebral compression fractures," *American Journal of Neuroradiology*, vol. 22, no. 2, pp. 366–372, 2001.
- [17] A. Baur, O. Dietrich, and M. Reiser, "Diffusion-weighted imaging of bone marrow: current status," *European Radiology*, vol. 13, no. 7, pp. 1699–1708, 2003.
- [18] S. Hwang and D. M. Panicek, "Magnetic resonance imaging of bone marrow in oncology, part 1," *Skeletal Radiology*, vol. 36, no. 10, pp. 913–920, 2007.
- [19] K. C. Lee, D. A. Bradley, M. Hussain et al., "A feasibility study evaluating the functional diffusion map as a predictive imaging biomarker for detection of treatment response in a patient with metastatic prostate cancer to the bone," *Neoplasia*, vol. 9, no. 12, pp. 1003–1011, 2007.
- [20] C. Reischauer, J. M. Froehlich, D.-M. Koh et al., "Bone metastases from prostate cancer: assessing treatment response by using diffusion-weighted imaging and functional diffusion maps—initial observations," *Radiology*, vol. 257, no. 2, pp. 523–531, 2010.
- [21] P. Lang, M. F. Wendland, M. Saeed et al., "Osteogenic sarcoma: noninvasive *in vivo* assessment of tumor necrosis with diffusion-weighted MR imaging," *Radiology*, vol. 206, no. 1, pp. 227–235, 1998.

